Fast oscillations localize the epileptogenic zone: an electrical source imaging study using high-density electroencephalography

Tamir Avigdor[1,2]; Chifaou Abdallah, MD[3]; Nicolás von Ellenrieder, PhD[4]; Annalisa Rubino[5]; Giorgio Lo Russo, MD[5]; Boris Bernhardt, PhD[4]; Lino Nobili, MD, PhD[6,7]; Christophe Grova, PhD[2,3,4]; Birgit Frauscher, MD, PD[1,8*]

1. Analytical Neurophysiology Lab, Montreal Neurological Institute and Hospital, McGill University, Montreal, Quebec, Canada.
2. Multimodal Functional Imaging Lab, Biomedical Engineering Department, McGill University
3. Multimodal Functional Imaging Lab, PERFORM Centre, Department of Physics, Concordia University, Montreal, QC, Canada.
4. Montreal Neurological Institute and Hospital, McGill University, Montreal, Quebec, Canada.
5. Claudio Munari Epilepsy Center, Niguarda Hospital, Milan, Italy.
6. Department of Neuroscience (DINOGMI), University of Genoa, Italy
7. IRCCS, Child Neuropsychiatry Unit, Instituto Giannina Gaslini, Genoa, Italy
8. Department of Medicine, Queens University, Kingston, ON, Canada

Running title: Fast oscillations & epileptogenic zone

Address of correspondence:
Birgit Frauscher, MD PD
Analytical Neurophysiology Lab
Montreal Neurological Institute & Hospital
McGill University
3801 University Street
Montreal, H3A 2B4, Quebec, Canada
Email: birgit.frauscher@mcgill.ca

ACKNOLWEGMENTS: This work is supported by the Department of Medicine Innovation Fund 2016 of Queen's University Internal Grant Competition to B.F. as well as a project grant of the Botterell-Howe-Powell Competition 2016 to B.F.. T.A.'s salary is supported by the Jenny Panitch Beckow Memorial Scholarship 2019-2020 of the Jewish Community Foundation of Montreal, start-up funding of the Montreal Neurological Institute to B.F. and a CIHR project grant MOP 401852 of C.G.. B.F.'s salary is supported by a salary award ("Chercheur-boursier clinicien

Junior 2”) 2018 – 2021 of the Fonds de Recherche du Québec – Santé. AR acknowledges the support of the Italian Ministry of Health - Targeted Research Grant RF-2010-2319316.

CONFLICTS OF INTEREST: None of the authors has any conflict of interested related to the submitted work.

ABSTRACT (245/250)

Fast Oscillations (FO) are a promising biomarker of the epileptogenic zone (EZ) in the intracranial electroencephalogram (EEG). Evidence using scalp EEG remains scarce. This is the first study that assesses if electrical source imaging of FO using 256-channel high-density EEG is feasible and useful for EZ identification. We analyzed high-density EEG recordings of 10 focal drug-resistant epilepsy patients with seizure-free postsurgical outcome (follow-up >2 years). We marked FO candidate events at the time of epileptic spikes and then verified them by screening for an isolated peak in the time-frequency plot. We performed electrical source imaging of FOs >40 Hz and spikes using the coherent Maximum Entropy of the Mean technique. Source localization maps were validated against the surgical cavity as approximation of the EZ. We identified FO events in 5 of the 10 patients. FOs were localizable in all 5 patients. The depth of the epileptic generator was either superficial or intermediate in all 5 patients with FO. The maximum of the FO maps was localized in the surgical cavity. We identified spikes in all 10 patients. Spikes were localized to the surgical cavity in 9 of 10 patients. In summary, FOs recorded with high-density EEG are able to localize the EZ. Our findings suggest that the presence of FOs co-localized with spikes points to a surface-close generator. These results can act as a proof of concept for future examination of FOs localization using scalp 256-channel high-density EEG as a viable marker of the EZ.

Key words: high-density electroencephalography, epilepsy, maximum entropy of the mean, electrical source imaging, non-invasive localization

INTRODUCTION

Epilepsy is a chronic condition characterized by recurrent seizures accompanied by negative impact on quality of life [Hinnell et al., 2010]. A significant number of 30% of patients with focal epilepsy are drug-resistant, and these numbers did not change over the past 30 years despite the development of multiple new antiepileptic drugs [Chen et al., 2018]. The therapy of choice for focal drug-resistant epilepsy is epilepsy surgery [Vakharia et al., 2018]. The aim of epilepsy surgery is to remove the epileptogenic zone (EZ) defined as the area of cortex that needs to be removed to achieve seizure freedom [Rosenow and Lüders, 2001]. In current praxis, the seizure-onset zone (SOZ) is used as the main proxy marker for the EZ. A sustained seizure-free condition is currently, however, obtained in only 50% of carefully selected patients [Krucoff et al., 2017; Mohan et al., 2018; West et al., 2019]. This is likely due to inaccurate localization of the EZ or a network involvement larger than initially expected [Englot, 2018]. This underlines the need to develop new markers and localization techniques for better identification of the EZ and hence improved surgical outcomes.

Recently, Fast Oscillations (FO) have been identified as promising novel interictal marker for the EZ [Frauscher et al., 2017]. Most evidence comes from intracranial EEG (iEEG) suggesting that resection of areas with high FO rates is associated with good surgical outcome, and that presence of FO after resection is predictive of postsurgical seizure relapse [Frauscher et al., 2017; Höller et al., 2015; van ’t Klooster et al., 2017; Jacobs et al., 2018; Tamilia et al., 2018]. In contrast, evidence from non-invasive methods is rather scarce [Thomschewski et al., 2019], and mainly obtained from magnetoencephalography (MEG). MEG studies from different centers suggest that it is possible to detect isolated FO events from interictal MEG recordings with satisfactory data quality [von Ellenrieder et al., 2016; van Klink et al., 2016a; Papadelis et al., 2016]. Four studies validated FO localization against the postsurgical cavity in good outcome patients as gold standard for the EZ; they point towards usefulness of FOs for delineating the EZ [van Klink et al., 2017; Velmurugan et al., 2019; Yin et al., 2019; Tamilia et al., 2020].

In contrast to MEG, high-density EEG (HD-EEG) would have the great advantage that it is widely available at epilepsy centers and more affordable given the high cost of operating a MEG device. From a technical point of view, however FO recording and localization using HD-EEG has even more challenges to overcome. The two main hurdles are a lower signal-to-noise ratio (SNR) due to attenuation of the signal by the skull in HD-EEG as well as a more complex solution of the forward problem needed for source localization given the necessity of assessing

accurately the conductivity of the head tissues, especially the skull [Goldenholz et al., 2009; de Munck et al., 2012; Hari and Puce, 2017; Ilmoniemi and Sarvas, 2019]. There is first evidence that FO can be detected also in the scalp EEG [Andrade-Valenca et al., 2011; Kobayashi et al., 2011; von Ellenrieder et al., 2012; Zelmann et al., 2014; van Klink et al., 2016b; Pizzo et al., 2016]. Some of these studies showed concordance with the area of the seizure-onset zone (SOZ) as determined by intracranial EEG or the resection cavity in patients with good seizure outcome [Kuhnke et al., 2018; Kuhnke et al., 2019; Tamilia et al., 2020]. Moreover, it was shown that presence of scalp FOs is associated with the depth of the epileptic generator, with FOs being present in case of more surface-close generators [Cuello-Oderiz et al., 2017]. Finally, it was suggested that scalp EEG might be superior for the detection of FOs due to higher rates of FOs detected in scalp EEG compared to MEG [van Klink et al., 2019, Tamilia et al., 2020]. Given the small size of the generators of FO [von Ellenrieder et al., 2014], HD-EEG might be superior to standard EEG. So far, there is only one study reporting scalp FOs using HD-EEG with 128 electrodes in the sensor space [Kuhnke et al., 2018].

In this study, we assessed the viability of detection and localization of FOs in epileptic patients using a HD-EEG array of 256 electrodes. We examined whether localization of FOs exceeding 40 Hz using HD-EEG is capable of delineating the EZ [Rosenow and Lüders, 2001]. We then compared results to those of spike source localization. For validation, we opted to use the surgical cavity in postsurgically seizure-free patients (Engel Ia) with a follow-up duration of > 2 years as best approximation of the EZ. We opted to not use the intracranially identified SOZ as alternative validation standard, given that a considerable number of patients do not become seizure-free after removal of the SOZ [Krucoff et al., 2017].

METHODS

Subjects' selection

A total of ten patients with seizure-free outcome > 2 years (Engel 1A [Engel, 1993]) were selected from the high-density EEG database of the Claudio Munari Epilepsy Center in Milan between 2015-2016. Selection criteria were presence of > 10 epileptic spikes during HD-EEG recording, recordings lasting 90 min on average, showing at least N2 sleep in order to have the least artifacts possible for FO detection [Zijlmans et al., 2017], absence of previous surgery, subsequent surgery with Engel 1a outcome and a minimum follow-up duration of 2 years,

availability of electrode positions and MRI co-registration, a minimum sampling rate of 500 Hz, as well as satisfactory data quality. Patient demographic and clinical information is provided in Table 1. The study conforms to the Declaration of Helsinki and was approved by Niguarda Hospital in Milan, Italy. A written informed consent was signed by all patients prior to study participation.

HD-EEG data acquisition and preprocessing

HD-EEG was recorded using a 256-electrode EGI system (Electrical Geodesic Incs, EGI, now Philips Neuro, Eugene, OR, USA) with a sampling rate of 500 Hz and hardware filter settings of 0.3 Hz for the high pass and 200 Hz for the low pass filter. The recording duration was approximately 1.5 h; this duration was chosen to enable the patient to fall asleep. The impedance was kept under 70 kOhm.

HD-EEG processing was performed with the Brainstorm software package [Tadel et al., 2011]. For interictal spike detection and analysis, preprocessing included 0.3–70 Hz band-pass filtering and DC correction (baseline window from −1000 ms to−500 ms before the marked spikes). No filter was applied for FO events.

The EEG sensor positions were estimated using digitalization with a SofTaxicOptic system (EMS s.r.l., Bologna, Italy). A linear coregistration with a pre-implant MRI (Achieva 1.5 T, Philips Healthcare) was performed. The digitized positions of the electrodes were then coregistered to the scalp surface segmented from the anatomical MRI of each patient, using a surface matching algorithm within the Brainstorm software. The HD-EEG electrodes located on the face and on the neck (approximately 40 channels) were excluded for further analysis in order to avoid artifacts caused by muscle or poor-contact electrodes [Hedrich et al., 2017].

Interictal event marking

Spikes were marked at their peak by an epileptologist (CA). All spike events occurring during N1, N2 or N3 sleep were screened for FO candidate events by a second epileptologist (BF). FO were defined as at least four oscillations clearly standing out of the background EEG in the gamma (40–80 Hz) and ripple (80-160 Hz) frequency band in the same electrodes as the spike that was marked at that time. FO candidate events were verified using a time-frequency plot screened for an isolated peak within the FO band (gamma or ripple) with no other visible peaks in the TF- plot in the same threshold within 0.5 s before and 0.5 s after (see Figure 1). TF plot

were computed using the Morlet wavelet with a central frequency of 1 Hz and a window duration of 3s and plotted as a power scale. We used this two-step approach in order to avoid misclassification of the filtering effect as “true” FOs. Given the low SNR of FOs, we attempted source localization only in patients with a minimum number of 5 FOs.

Electrical source imaging

The 1.5T anatomical MRI was segmented, and the cortical surface was obtained using the FreeSurfer software package (v=6.0, http://surfer.nmr.mgh.harvard.edu). The EEG forward problem was solved using the boundary element method (BEM) [Kybic et al., 2006]. The gain matrix was calculated using a 3-layer BEM model for brain, skull and scalp (conductivity of 0.33, 0.0165, 0.33 S/m respectively) using OpenMEEG [Gramfort et al., 2010] implemented in the Brainstorm software. The inverse problem was solved using the Maximum Entropy on the Mean (MEM) method [Amblard et al., 2004]. MEM uses a Bayesian approach, which introduces a multivariate source prelocalization in which the brain is divided into K parcels. Later the MEM solver uses the multivariate source prelocalization coefficient as a hidden variable for the reference distribution for the activation probability of each parcel. This property enables MEM to switch off parcels, to which it attributes no contributing value to the solution.

MEM is a nonlinear distributed inverse problem method, which makes use of a data-driven parcellation (DDP) technique in order to cluster the data into K parcels [Lapalme et al., 2006]. This is used in the multivariate source pre-localization (MSP) method [Mattout et al., 2005] which is a projection method that estimates a coefficient, which characterizes the possible contribution of each dipolar source to the data. We make use of it in the MEM reference model, in which a hidden variable is associated to each parcel in order to model the probability of the parcel to be active or to be switched off [Chowdhury et al., 2013; Chowdhury et al., 2016; Hedrich et al., 2017; Pellegrino et al., 2018]. The wMEM extension of the MEM framework [Lina et al., 2014] decomposes the signal in a discrete wavelet basis before performing MEM source localization on each time–frequency box. Thus, wMEM is particularly suited to localize oscillatory patterns, as evaluated with realistic simulations, but also when localizing FOs [Kybic et al., 2006; von Ellenrieder et al., 2016] and oscillatory patterns at seizure onset [Pellegrino et al., 2016]. Two different variations of MEM were used in this study: wavelet MEM (wMEM) was adopted to localize FOs, whereas coherent MEM (cMEM) was adopted to localize spikes. We used the standard settings of the wMEM and cMEM as provided in Brainstorm [Chowdhury et al., 2013; Lina et al., 2014], except that for wMEM we set the amount of vanishing moments for

the Daubechies wavelet to 8. The use of 8 vanishing moments instead of the default 4 was done in order to capture the complexity of FOs. The baseline to model the diagonal noise covariance matrix for both wMEM and cMEM was chosen for each patient visually during an artifact- and spike-free 2-second period. wMEM was performed on the marked duration of the FO by selecting the only time-frequency box exhibiting the largest amount of energy as recommended [Kybic et al., 2006; von Ellenrieder et al., 2016]. The spike map was computed for -50 to +50 ms from the spike peak using cMEM.

IEDs and FO Consensus maps

In order to take into account reliability and reproducibility between epileptic discharges to be localized (IEDs or FOs), we applied the concept of consensus maps of source localization [Chowdhury et al., 2018]. In order to estimate these consensus maps for every patient, we first applied cMEM or wMEM to generate source maps of all single events, FO or spike events. In a second step, we estimated a similarity index between all single event source maps (FOs or spikes), based on spatio-temporal correlation around the peak of the event The source maps were then clustered using a hierarchical clustering approach (Ward's hierarchical clustering) followed by thresholding of the dendrogram to obtain the optimal number of clusters. This consensus approach was considered instead of simple averaging of the event followed by one source localization, in order to enhance reliability between source localization results and reducing the influence of more noisy maps. We previously carefully demonstrated the robustness of this approach when considering either EEG source imaging, MEG source imaging or EEG-MEG fusion source imaging [Chowdhury et al., 2018].

Generator depth

The depth of the generator was assessed on the basis of all available clinical information. The generator depth was divided into 3 categories: superficial, intermediate and deep as done in previous work [Cuello-Oderiz et al., 2017]. Superficial was considered as involving the neocortex adjacent to the skull including the bottom of the sulcus; deep, was considered as involving the medial aspects of the frontal, parietal, occipital, and temporal lobes and temporo-occipital basal regions; and intermediate, generators found in regions not fitting the above two categories.

Metrics & Statistics

Final maps were thresholded at 50% of the maximum reconstructed intensity for both visualization and statistical purposes. We previously demonstrated that MEM source localization results provide maps with high contrast, therefore results on the spatial extent are relatively stable within a large range of detection threshold, as opposed to other standard source localization techniques [Chowdhury et al., 2018; Pellegrino et al., 2018; Pellegrino et al., 2019]. In order to assess the success or failure of the localization, we considered the surgical cavity as a reference. Since all selected patients are > 2 year postsurgically seizure-free (Engel 1a), we are sure that the presumed epileptogenic zone was indeed localized within the cavity. The surgical cavity was fitted as a surface-based region of interest (scout) on the brain source model (see Supplementary Figure 1). This was done visually using the post-surgical MRI co-registered to the intact cortical surface of the pre-surgical MRI, using the Brainstorm software. The coregistration between presurgical and postsurgical MRI was obtained with a 6 parameter rigid body coregistration using the MINC toolkit (https://bic-mni.github.io/). All evaluation metrics were then estimated using this scout of the surgical cavity as our clinical reference. We assessed the following validation metrics: the minimum Distance Localization Error (Dmin), Spatial Dispersion (SD), the spatial Map Overlap (MO), and Signal to Noise Ratio (SNR).

- Dmin: the minimum distance localization error was computed as the distance in mm from the maximum of the map to the closest vertex belonging to the cavity. Whenever this maximum was located inside the cavity, Dmin was set to 0 mm.

- Spatial Dispersion (SD): the SD was computed as the sum of the localization map with acitivity with either no threshold (Fig. 4) or 50% threshold (Fig. 2) weighted by its distance from the scout's nearest point.

- Spatial Map Overlap (MO): MO was defined as the percentage of the localization map with either no threshold (Fig. 4) or 50% threshold (Fig. 2) in the scout such that if all the localization is inside then it equals 100% overlap.

- Signal to noise ratio (SNR): the SNR was calculated using the mean amplitude at the time of the event divided by the standard deviation of a baseline period of 10 ms long for 200ms prior to the event, the calculation was done on the filtered signal for each type of event (0.3-70Hz for spikes and 40-80Hz for FOs). For spikes the calculation was made on the average spike and for FOs each event was calculated then the average for each patient then between patients to reach the final SNR (SNRs are shown in normalized units, not in dB).

For each of the validation metrics described above, we considered only the best as defined by the cluster with the highest number of events cluster for both spikes and FOs i.e after clustering all the events for each type event (spike or FO) only the one with highest event numbers was selected for further analysis. We used the Welch's t-test as not every patient had FOs thus creating unequal groups. The Fisher exact test was used to assess the distribution of generator depth categories between patients with and without FOs.

RESULTS

Detection of FOs

FOs in the gamma band (40-80 Hz) were found in five of the ten patients (Table 2). The mean number of FOs was 12.2±3.9 (range, 10-20) with a mean SNR of 3.4±1.4. Figure 1 shows representative examples of FOs of the 5 patients in the unfiltered signal, the filtered signal, as well as the time frequency plot. Spikes were present in all ten patients. The mean number of spikes was 99.6±99.1 (range, 12-303) with a mean SNR of 9.3±2.7. As expected, the SNR was significantly lower in FOs than in spikes ($p<0.05$).

Electrical source imaging

FO sources were localized in 5 out of 5 patients inside the surgical cavity (Figure 2 B) resulting in a minimum distance Dmin of 0 mm. Source maps were localized within the surgical cavity with an SD of 9.4±3.2 mm and an MO of 62.0±15.0%. Spike sources localized inside the surgical cavity in 9 out of 10 patients (Figure 2 D and Suppl. Figure 2) with a Dmin of 6.45±20.41 mm. Source maps were localized within the surgical cavity with an SD of 6.2±10.9 mm and an MO of 76.0±30.0%. The spread outside the cavity as well as the activation overlap with the surgical cavity did not differ significantly between FOs and spikes (SD: $p=0.17$; MO: $p=0.09$). For further details see Figure 3.

Usefulness of the consensus map approach for FO source localization

The consensus map approach for FOs sources resulted in less disperse maps compared to the one obtained by simply averaging of all FO maps (SD difference between cluster versus averaged map: 10.3±4.8mm versus 9.4±3.2mm; $p=0.4$). This difference in SD became significant when no thresholding was considered prior to the estimation of SD, resulting in a SD

of 18.1±3.1mm for the averaged map compared to 16.3±3.2 mm for the consensus map (p=0.007). This demonstrated that the hierarchical clustering approach considered for the consensus map helped to remove the impact of more noisy FO events, resulting in a more reliable localization. This is illustrated in Figure 4, which shows only the activations outside the cavity for averaged versus consensus FO source maps, when no threshold is applied.

Generator depth

We found that all patients with localizable FOs actually had a surface close generator, with 4 patients being classified as having a superficial generator and 1 patient being classified as having an intermediate generator (Table 2). In the 5 patients not showing sufficient numbers of localizable FOs, the generator proved to be deep in 4 cases and intermediate in 1 (p=0.02). In the patient in whom the spike map localized outside the surgical cavity, the generator was actually localized in the cingulate gyrus, which is a deep region usually not detectable from scalp EEG.

DISCUSSION

This study presents promising results of electrical source imaging of FOs for identification of the EZ in patients with drug-resistant focal epilepsy using high-density EEG. We demonstrated that (i) FOs can be recorded in scalp high-density EEG during short recording sessions lasting 90 minutes, (ii) the presence or absence of sufficient numbers of FOs is dependent on the depth of the epileptic generator, and (iii) electrical source imaging of FOs is feasible and able to correctly localize the EZ.

Use of FOs for identification of the EZ

FOs were present in 50% of the investigated patients despite only short segments with light sleep used for detection of FOs. Interestingly all patients exhibiting FOs and spikes had a surface-close generator, whereas the patients in whom we did not identify FOs but only spikes had an either intermediate or deep generator. This finding is in keeping with a previous study investigating high-frequency oscillations in the scalp demonstrating that scalp FOs are correlated with the depth of the epileptic generator [Cuello Oderiz et al., 2017].

We found that the maxima of the electrical source localization maps of FOs correctly localized the EZ as approximated by the surgical cavity in all patients. The ability of FOs to non-invasively localize the EZ was recently demonstrated using MEG [von Ellenrieder et al., 2016; Nissen et al., 2016; Velmurugan et al., 2019; Yin et al., 2019; Tamilia et al., 2020]. Velmurugan and colleagues [2019] have recently shown the utility of high-frequency oscillations in correctly localizing the EZ in MEG in 52 patients thus demonstrating its potential as a scalp biomarker. Yet, while MEG has advantages such as better SNR and less complicated head modeling impacting spatial resolution when compared to EEG [Ilmoniemi and Sarvas, 2019], the lack of availability in most centers and its high maintenance cost makes it less ideal as a tool for everyday use in presurgical evaluation. In addition, it is worth noting that while EEG has been shown to detect higher numbers of FOs [van Klink et al., 2019, Tamilia et al., 2020], spatial coverage is key due to the low SNR and a high-density array is preferable. Thus, this proof of principle study using HD-EEG with 256 electrodes together with the already existing evidence in MEG and EEG [Thomschewsky et al., 2019; van Klink et al., 2019, Tamilia et al., 2020] points to HD-EEG being a feasible candidate for FO localization of the EZ during pre-surgical evaluation.

Comparison of FO to spike sources

When comparing FO to spike source localization, we found that FO source localization and spike source localization were concordant with the latter resulting in localizations in all ten study subjects. Note is made that one of the spike localizations was outside and far from the epileptic generator. The patient was identified as having a deep generator in the posterior cingulate gyrus determined by a focal MRI lesion and PET hypometabolism, and the spikes we localized along the cortical surface corresponded hence to propagated activity. In this patient, FOs were absent suggesting that source localization results in presence of FOs are very likely pointing to the “true” onset generator [Cuello-Oderiz et al., 2017], whereas absence of FOs might constitute a red flag for propagated activity [Plummer et al., 2019]. Our finding might hence be able to address a longstanding problem inherent to non-invasive source localization. However, careful evaluation of propagation of source localization along the peak of the spike vs. FOs localization was out of the scope of this study and will be considered in future investigations.

Different measures for source localization quality

In clinical practice most studies assessed the concordance of the source with the assumed EZ at the lobar level [Duez et al., 2019; Rampp et al., 2019], or at best at the sub-lobar level [Heers

et al., 2016]. We evaluated our findings using different quantitative validation metrics, several of them being similar to the ones proposed in Pellegrino et al. [2018] and Chowdhury et al. [2018] in order to assess the quality of our results as objectively as possible regarding the source map maxima, its spatial extent, and the spatial overlap with the resection cavity. The originality of our proposed approach was also to consider an accurate delineation of the resection cavity as our reference for the evaluation of source localization results, whereas such a comparison was more qualitative in other studies [Abdallah et al., 2017]. The accuracy of FOs localization was high with the maxima localized to the surgical cavity in all patients. Albeit being not significant, the extent of the source seemed to be more widespread in FOs compared to spikes. However, whereas the estimation of the spatial extent of spike maps with cMEM has been carefully evaluated by our group [Chowdhury et al., 2016; Pellegrino et al., 2016; Pellegrino et al., 2018], the evaluation of the spatial extent of wMEM for FOs would require further careful investigation. Moreover, it is difficult to disentangle whether the spatial extent of FOs maps was true extent or only resulted from the localization of low SNR events. This might be potentially explained by the small number of FOs given the short recording time of 90 minutes, as well as by the lack of consolidated sleep in the present study; longer recording durations preferably overnight are likely to be more favorable regarding FO quantity and SNR. Future research performing prolonged overnight sleep recordings is awaited for confirmation.

Importance of consensus map approach for FO source maps

In this study we applied for the first time for spike and FOs in HD-EEG the consensus map approach we recently proposed as a more robust approach than events averaging to provide reliable source localization, while taking into account the reproducibility of single discharges source maps [Chowdhury et al., 2018]. In this study, this was our first attempt to consider consensus maps from wMEM results for FO localization. We therefore first performed a single event FO source localization, using only the time-frequency box exhibiting the largest amount of energy along the FOs, following the exact same methodology proposed in MEG by our group [von Ellenrieder et al., 2016; Chowdhury et al., 2018]. We then compared every single FO source map using a hierarchical clustering in order to separate the data from events that were not in agreement with the majority of events and which would therefore add noise to the maps, as done in our previous work for spikes [Chowdhury et al., 2018]. This consensus map approach seems to be particularly useful for FOs, which in case of a discordant FO event tend to create a noisier map. Figure 4 shows a significant improvement of source localization of FOs using this consensus map approach, when compared to standard averaging of all FO maps,

resulting in a reduction of the SD of the source map outside the presumed EZ as approximated by the surgical cavity. If the fact of a lower accuracy of 0.87 in a recent combined EEG/MEG study [Tamilia et al., 2020] can be explained by the advantage that a consensus map could offer or our better spatial coverage with 256 electrodes compared to 70 electrodes awaits further evaluation.

cMEM and wMEM for source localization of epileptic discharges

Most previous work in source localization of FOs in MEG used the Beamformer technique, as it is assumed to be able to detect distributed and deep sources [Hu et al., 2017]. Yet Beamformer is not a source localization method in its proper sense, but corresponds rather to a statistical dipole scanning approach, iteratively assessing how likely it would be to fit an equivalent current dipole at a specific position in a 3D grid covering the brain [Hillebrand et al., 2005]. One important feature of the Beamforming technique is its inherent denoising properties [Cheyne et al., 2007; Hillebrand et al., 2005], as a spatial filtering approach, which is probably the main reason why several groups have considered this localization approach for FOs [Belardinelli et al., 2012]. In this study, we chose the MEM framework, as one of the only distributed approaches that has been proposed to carefully recover the generators of epileptic discharges together with their spatial extent [Birot et al., 2011; Chowdhury et al., 2016]. We also considered the time-frequency based extension of MEM (wMEM), providing us with the unique property of localization in the frequency domain [Lina et al., 2014], thus making it a good tool for the localization of oscillatory events, as previously demonstrated for FOs in MEG and low-density EEG [von Ellenrieder et al., 2016; Tamilia et al., 2020], localization of oscillatory patterns at the seizure onset in EEG and MEG [Pellegrino et al., 2016; Pellegrino et al., 2018] and ongoing MEG resting state fluctuations [Aydin et al., 2020 in minor revision]. Careful comparison of FOs using wMEM or beamforming will be important to consider on larger populations in future investigations but was beyond the scope of this clinically oriented study.

SNR as a technical challenge

The SNR of EEGs can vary widely with different conditions as it is very susceptible to muscle artifact notably as well as interferences with outside noise [Islam et al., 2016]. This latter challenge might be potentially overcome by the use of a low-noise amplifier [Fedele et al., 2015], which could make it possible to obtain low noise recordings in the future. Prolonged clean recordings can be extremely valuable for FO identification, as data have the least artifacts

in the high-frequency domain during sleep [Zijlmans et al., 2017]. Yet in the case of prolonged recordings it might not be feasible to visually mark and validate each FO and a computational approach might be needed [Höller et al., 2018]. Another interesting aspect that might influence the results is the type of electrode being used. Recent research demonstrated that tripolar EEG electrodes might yield some benefit with higher signal quality [Toole et al., 2019].

Limitations

First, we would like to acknowledge that our sample size is small. However, all 10 patients selected for this study were postsurgically seizure-free with an at least 1 year postsurgical follow-up, which allowed us to have the best estimate possible for approximation of the EZ in this proof-of-principle study. An alternative would have been to validate against the intracranially identified SOZ [Papadelis et al., 2016; Kuhnke et al., 2018; Dirodi et al., 2019]. Given however, that up to ~50 % of patients in whom the SOZ has been surgically removed, do not become seizure-free after surgery [Krucoff et al., 2017] , this seemed to us to not be the best option for the validation of our approach, even though a large resection diminishes the sensitivity to the real EZ (see patient 1 for an example). Second, we only had short recordings of approximately 1.5 h, during which patients achieved mostly only light sleep. Prolonged recordings of overnight sleep as planned in future research could result in higher patient numbers in whom FOs can be identified and results regarding the extent of the source might be improved given higher event numbers and therefore better SNR. Third, we marked FOs at the time of spikes as suggested by other authors [Nissen et al., 2016; Velmurugan et al., 2019], as FOs at the time of spikes have a greater chance of a correct localization than FOs occurring independent of spikes [Dirodi et al., 2019]. To avoid a confound with a filtering effect of spikes [Bénar et al., 2010], we followed a two-step procedure to exclude false positives based on both visual signal inspection and presence of an isolated peak in the time-frequency representation in order to avoid misclassification of FOs.

This study demonstrated the ability of 256-channel HD-EEG to correctly identify the EZ using source localization of FOs. Presence or absence of FOs was shown to be dependent on the presence of a surface close generator. This points to an added value of FO source localization, as presence of concordant spike and FO sources could confirm correct localization of the EZ, whereas lack of FO sources might point to the fact that the identified spike source could be the correlate of rather propagated activity and not the primary source, a problem inherent to non-invasive source imaging. Future research is needed with a larger cohort of patients and longer

recording durations with consolidated sleep for improved data quality in order to further validate the viability of the use of scalp FOs for clinical decision making.

DATA AVAILABILITY STATEMENT

The data that support the findings of this study are available from the corresponding author upon reasonable request.

REFERENCES

Abdallah C, Maillard LG, Rikir E, Jonas J, Thiriaux A, Gavaret M, Bartolomei F, Colnat-Coulbois S, Vignal J-P, Koessler L (2017): Localizing value of electrical source imaging: Frontal lobe, malformations of cortical development and negative MRI related epilepsies are the best candidates. Neuroimage Clin 16:319–329.

Andrade-Valenca L, Dubeau F, Mari F, Zelmann R, Gotman J (2011): Interictal scalp fast oscillations as a marker of the seizure onset zone. Neurology 77:524-31.

Amblard C, Lapalme E, Lina J-M (2004): Biomagnetic source detection by maximum entropy and graphical models. IEEE Trans Biomed Eng 51:427–442.

Aydin Ü, Pellegrino G, Bin Ka'b Ali O, et al. (2020): Magnetoencephalography resting state connectivity patterns as indicatives of surgical outcome in epilepsy patients. J Neural Eng 2020, in press.

Belardinelli P, Ortiz E, Barnes G, Noppeney U, Preissl H (2012): Source reconstruction accuracy of MEG and EEG Bayesian inversion approaches. PLoS One 7:e51985.

Bénar CG, Chauvière L, Bartolomei F, Wendling F (2010): Pitfalls of high-pass filtering for detecting epileptic oscillations: a technical note on “false” ripples. Clin Neurophysiol 121:301–310.

Birot G, Albera L, Wendling F, Merlet I (2011): Localization of extended brain sources from EEG/MEG: the ExSo-MUSIC approach. Neuroimage 56:102–113.

Chen Z, Brodie MJ, Liew D, Kwan P (2018): Treatment Outcomes in Patients With Newly Diagnosed Epilepsy Treated With Established and New Antiepileptic Drugs: A 30-Year Longitudinal Cohort Study. JAMA Neurol 75:279–286.

Cheyne D, Bostan AC, Gaetz W, Pang EW (2007): Event-related beamforming: a robust method for presurgical functional mapping using MEG. Clin Neurophysiol 118:1691–1704.

Chowdhury RA, Lina JM, Kobayashi E, Grova C (2013): MEG source localization of spatially extended generators of epileptic activity: comparing entropic and hierarchical bayesian approaches. PLoS One 8:e55969.

Chowdhury RA, Merlet I, Birot G, Kobayashi E, Nica A, Biraben A, Wendling F, Lina JM, Albera L, Grova C (2016): Complex patterns of spatially extended generators of epileptic activity: Comparison of source localization methods cMEM and 4-ExSo-MUSIC on high resolution EEG and MEG data. Neuroimage 143:175–195.

Chowdhury RA, Pellegrino G, Aydin Ü, Lina J-M, Dubeau F, Kobayashi E, Grova C (2018): Reproducibility of EEG-MEG fusion source analysis of interictal spikes: Relevance in presurgical evaluation of epilepsy. Hum Brain Mapp 39:880–901.

Cuello-Oderiz C, von Ellenrieder N, Dubeau F, Gotman J (2017): Influence of the location and type of epileptogenic lesion on scalp interictal epileptiform discharges and high-frequency oscillations. Epilepsia 58:2153–2163.

de Munck J, Wolters C, Clerc M. 2012 EEG & MEG forward modeling. In: Handbook of Neural Activity Measurement, edited by Brette R, Destexhe A. New York, NY: Cambridge Univ Press.

Dirodi M, Tamilia E, Grant PE, Madsen JR, Stufflebeam SM, Pearl PL, Papadelis C (2019): Noninvasive Localization of High-Frequency Oscillations in Children with Epilepsy: Validation against Intracranial Gold-Standard. Conf Proc . Annu Int Conf IEEE Eng Med Biol Soc IEEE Eng Med Biol Soc Annu Conf 2019:1555–1558.

Duez L, Tankisi H, Hansen PO, Sidenius P, Sabers A, Pinborg LH, Fabricius M, Rásonyi G, Rubboli G, Pedersen B, Leffers A-M, Uldall P, Jespersen B, Brennum J, Henriksen OM, Fuglsang-Frederiksen A, Beniczky S (2019): Electromagnetic source imaging in presurgical workup of patients with epilepsy: A prospective study. Neurology 92:e576–e586.

Engel J Jr, Van Ness PC, Rasmussen TB, Ojemann LM. (1993) Outcome with respect to epileptic seizures. Second edition. In: Engel J Jr, editor. Surgical Treatment of the Epilepsies. New York: Raven Press, LTD; p. 609–21.

Englot DJ (2018): A modern epilepsy surgery treatment algorithm: Incorporating traditional and emerging technologies. Epilepsy Behav 80:68–74.

Fedele T, Scheer HJ, Burghoff M, Curio G, Körber R (2015): Ultra-low-noise EEG/MEG systems enable bimodal non-invasive detection of spike-like human somatosensory evoked responses at 1 kHz. Physiol Meas 36:357–368.

Frauscher B, Bartolomei F, Kobayashi K, Cimbalnik J, van ’t Klooster MA, Rampp S, Otsubo H, Höller Y, Wu JY, Asano E, Engel J Jr, Kahane P, Jacobs J, Gotman J (2017): High-frequency oscillations: The state of clinical research. Epilepsia 58:1316–1329.

Goldenholz DM, Ahlfors SP, Hämäläinen MS, Sharon D, Ishitobi M, Vaina LM, Stufflebeam SM (2009): Mapping the signal-to-noise-ratios of cortical sources in magnetoencephalography and electroencephalography. Hum Brain Mapp 30:1077–1086.

Gramfort A, Keriven R, Clerc M (2010): Graph-based variability estimation in single-trial event-related neural responses. IEEE Trans Biomed Eng 57:1051–1061.

Harri R, Puce A (2017): MEG-EEG Primer. Oxford University Press.

Heers M, Chowdhury RA, Hedrich T, Dubeau F, Hall JA, Lina JM, Grova C, Kobayashi E (2016). Localization accuracy of distributed inverse solutions for electrical and magnetic source imaging of interictal epileptic discharges in patients with focal epilepsy. Brain Topogr 29:162-81.

Hedrich T, Pellegrino G, Kobayashi E, Lina JM, Grova C (2017): Comparison of the spatial resolution of source imaging techniques in high-density EEG and MEG. Neuroimage 157:531–544.

Hillebrand A, Singh KD, Holliday IE, Furlong PL, Barnes GR(2005): A new approach to neuroimaging with magnetoencephalography. Hum Brain Mapp 25:199–211.

Hinnell C, Williams J, Metcalfe A, Patten SB, Parker R, Wiebe S, Jetté N (2010): Health status and health-related behaviors in epilepsy compared to other chronic conditions--a national population-based study. Epilepsia 51:853–861.

Höller P, Trinka E, Höller Y (2018): High-Frequency Oscillations in the Scalp Electroencephalogram: Mission Impossible without Computational Intelligence. Comput Intell Neurosci 2018:1638097.

Höller Y, Kutil R, Klaffenböck L, Thomschewski A, Höller PM, Bathke AC, Jacobs J, Taylor AC, Nardone R, Trinka E (2015): High-frequency oscillations in epilepsy and surgical outcome. A meta-analysis. Front Hum Neurosci 9:574.

Hu Y, Lin Y, Yang B, Tang G, Liu T, Wang Y, Zhang J (2017): Deep Source Localization with Magnetoencephalography Based on Sensor Array Decomposition and Beamforming. Sensors 17 .

Ilmoniemi RJ, Sarvas J (2019): Brain Signals: Physics and Mathematics of MEG and EEG. MIT Press.

Islam MK, Rastegarnia A, Yang Z (2016): Methods for artifact detection and removal from scalp EEG: A review. Neurophysiol Clin 46:287–305.

Jacobs J, Wu JY, Perucca P, Zelmann R, Mader M, Dubeau F, Mathern GW, Schulze-Bonhage A, Gotman J (2018): Removing high-frequency oscillations: A prospective multicenter study on seizure outcome. Neurology 91:e1040–e1052.

Kobayashi K, Yoshinaga H, Toda Y, Inoue T, Oka M, Ohtsuka Y (2011): High-frequency oscillations in idiopathic partial epilepsy of childhood. Epilepsia 52:1812–1819.

Krucoff MO, Chan AY, Harward SC, Rahimpour S, Rolston JD, Muh C, Englot DJ (2017): Rates and predictors of success and failure in repeat epilepsy surgery: A meta-analysis and systematic review. Epilepsia 58:2133–2142.

Kuhnke N, Klus C, Dümpelmann M, Schulze-Bonhage A, Jacobs J (2019): Simultaneously recorded intracranial and scalp high frequency oscillations help identify patients with poor postsurgical seizure outcome. Clin Neurophysiol 130:128–137.

Kuhnke N, Schwind J, Dümpelmann M, Mader M, Schulze-Bonhage A, Jacobs J (2018): High Frequency Oscillations in the Ripple Band (80-250 Hz) in Scalp EEG: Higher Density of Electrodes Allows for Better Localization of the Seizure Onset Zone. Brain Topogr 31:1059–1072.

Kybic J, Clerc M, Faugeras O, Keriven R, Papadopoulo T (2006): Generalized head models for MEG/EEG: boundary element method beyond nested volumes. Phys Med Biol 51:1333–46.

Lapalme E, Lina J-M, Mattout J (2006): Data-driven parceling and entropic inference in MEG. Neuroimage 30:160–171.

Lina JM, Chowdhury R, Lemay E, Kobayashi E, Grova C (2014): Wavelet-based localization of oscillatory sources from magnetoencephalography data. IEEE Trans Biomed Eng 61:2350–2364.

Mattout J, Pélégrini-Issac M, Garnero L, Benali H (2005): Multivariate source prelocalization (MSP): use of functionally informed basis functions for better conditioning the MEG inverse problem. Neuroimage 26:356–373.

Mohan M, Keller S, Nicolson A, Biswas S, Smith D, Osman Farah J, Eldridge P, Wieshmann U (2018): The long-term outcomes of epilepsy surgery. PLoS One 13:e0196274.

Nissen IA, van Klink NEC, Zijlmans M, Stam CJ, Hillebrand A (2016): Brain areas with epileptic high frequency oscillations are functionally isolated in MEG virtual electrode networks. Clin Neurophysiol 127:2581–2591.

Papadelis C, Tamilia E, Stufflebeam S, Grant PE, Madsen JR, Pearl PL, Tanaka N (2016): Interictal High Frequency Oscillations Detected with Simultaneous Magnetoencephalography and Electroencephalography as Biomarker of Pediatric Epilepsy. J Vis Exp. (118);54883

Pellegrino G, Hedrich T, Chowdhury R, Hall JA, Lina J-M, Dubeau F, Kobayashi E, Grova C (2016): Source localization of the seizure onset zone from ictal EEG/MEG data. Hum Brain Mapp 37:2528–2546.

Pellegrino G, Hedrich T, Chowdhury RA, Hall JA, Dubeau F, Lina J-M, Kobayashi E, Grova C (2018): Clinical yield of magnetoencephalography distributed source imaging in epilepsy: A comparison with equivalent current dipole method. Hum Brain Mapp 39:218–231.

Pellegrino G, Hedrich T, Porras-Bettancourt M, Lina J-M, Grova C, Kobayashi E (2019): Accuracy and spatial properties of distributed magnetic source imaging (dMSI) techniques in the investigation of focal epilepsy patients. Clinical Neurophysiology.130;8-e117

Pizzo F, Frauscher B, Ferrari-Marinho T, Amiri M, Dubeau F, Gotman J (2016): Detectability of Fast Ripples (>250 Hz) on the Scalp EEG: A Proof-of-Principle Study with Subdermal Electrodes. Brain Topogr 29:358–367.

Plummer C, Vogrin SJ, Woods WP, Murphy MA, Cook MJ, Liley DTJ (2019): Interictal and ictal source localization for epilepsy surgery using high-density EEG with MEG: a prospective long-term study. Brain 142:932–951.

Rampp S, Stefan H, Wu X, Kaltenhäuser M, Maess B, Schmitt FC, Wolters CH, Hamer H, Kasper BS, Schwab S, Doerfler A, Blümcke I, Rössler K, Buchfelder M (2019): Magnetoencephalography for epileptic focus localization in a series of 1000 cases. Brain 142:3059–3071.

Rosenow F, Lüders H (2001): Presurgical evaluation of epilepsy. Brain 124:1683–1700.

Tadel F, Baillet S, Mosher JC, Pantazis D, Leahy RM (2011): Brainstorm: a user-friendly application for MEG/EEG analysis. Comput Intell Neurosci 2011:879716.

Tamilia E, Park E-H, Percivati S, Bolton J, Taffoni F, Peters JM, Grant PE, Pearl PL, Madsen JR, Papadelis C (2018): Surgical resection of ripple onset predicts outcome in pediatric epilepsy. Ann Neurol 84:331–346.

Tamilia E, Dirodi M, Alhilani M, Grant PE, Madsen JR, Stufflebeam SM, Pearl PL, Papadelis C (2020): Scalp ripples as prognostic biomarkers of epileptogenicity in pediatric surgery. Ann Clin Transl Neurol:acn3.50994.

Thomschewski A, Hincapie AS, Frauscher B (2019): Localization of the epileptogenic zone using high frequency oscillations. Front Neurol 10:94.

Toole C, Martinez-Juárez IE, Gaitanis JN, Sunderam S, Ding L, DiCecco J, Besio WG (2019): Source localization of high-frequency activity in tripolar electroencephalography of patients with epilepsy. Epilepsy Behav 101:106519.

Vakharia VN, Duncan JS, Witt J-A, Elger CE, Staba R, Engel J Jr (2018b): Getting the best outcomes from epilepsy surgery. Ann Neurol 83:676–690.

van Klink N, Hillebrand A, Zijlmans M (2016a): Identification of epileptic high frequency oscillations in the time domain by using MEG beamformer-based virtual sensors. Clin Neurophysiol 127:197–208.

van Klink N, Frauscher B, Zijlmans M, Gotman J (2016b): Relationships between interictal epileptic spikes and ripples in surface EEG. Clin Neurophysiol 127:143–149.

van Klink N, van Rosmalen F, Nenonen J, Burnos S, Helle L, Taulu S, Furlong PL, Zijlmans M, Hillebrand A (2017): Automatic detection and visualisation of MEG ripple oscillations in epilepsy. Neuroimage Clin 15:689–701.

van Klink N, Mooij A, Huiskamp G, Ferrier C, Braun K, Hillebrand A, Zijlmans M (2019): Simultaneous MEG and EEG to detect ripples in people with focal epilepsy. Clin Neurophysiol 130:1175–1183.

van ’t Klooster MA, van Klink NEC, Zweiphenning WJEM, Leijten FSS, Zelmann R, Ferrier CH, van Rijen PC, Otte WM, Braun KPJ, Huiskamp GJM, Zijlmans M (2017): Tailoring epilepsy surgery with fast ripples in the intraoperative electrocorticogram. Ann Neurol 81:664–676.

Velmurugan J, Nagarajan SS, Mariyappa N, Mundlamuri RC, Raghavendra K, Bharath RD, Saini J, Arivazhagan A, Rajeswaran J, Mahadevan A, Malla BR, Satishchandra P, Sinha S (2019): Magnetoencephalography imaging of high frequency oscillations strengthens presurgical localization and outcome prediction. Brain 142:3514–3529.

von Ellenrieder N, Andrade-Valença LP, Dubeau F, Gotman J (2012): Automatic detection of fast oscillations (40-200Hz) in scalp EEG recordings. Clin Neurophysiol 123:670–680.

von Ellenrieder N, Beltrachini L, Perucca P, Gotman J (2014): Size of cortical generators of epileptic interictal events and visibility on scalp EEG. Neuroimage 94:47–54.

von Ellenrieder N, Pellegrino G, Hedrich T, Gotman J, Lina J-M, Grova C, Kobayashi E (2016): Detection and Magnetic Source Imaging of Fast Oscillations (40-160 Hz) Recorded with Magnetoencephalography in Focal Epilepsy Patients. Brain Topogr 29:218–231.

West S, Nevitt SJ, Cotton J, Gandhi S, Weston J, Sudan A, Ramirez R, Newton R (2019): Surgery for epilepsy. Cochrane Database Syst Rev 6:CD010541.

Yin C, Zhang X, Chen Z, Li X, Wu S, Lv P, Wang Y (2019): Detection and localization of interictal ripples with magnetoencephalography in the presurgical evaluation of drug-resistant insular epilepsy. Brain Res 1706:147–156.

Zelmann R, Lina JM, Schulze-Bonhage A, Gotman J, Jacobs J (2014): Scalp EEG is not a blur: it can see high frequency oscillations although their generators are small. Brain Topogr 27:683–704.

Zijlmans M, Worrell GA, Dümpelmann M, Stieglitz T, Barborica A, Heers M, Ikeda A, Usui N, Le Van Quyen M (2017): How to record high-frequency oscillations in epilepsy: A practical guideline. Epilepsia 58:1305–1315.

TABLES & FIGURES

Table 1. Demographic and clinical information of the study sample.

#	Sex	Age	Epilepsy type	Epilepsy onset (years)	EEG ictal	EEG interictal	MRI	Surgery	Pathology
Patients with FOs									
1	W	10	TPO	3	R T	R PT	R hemisphere atrophy with suprasylvian maximum	TPO disconnection	gliosis
2	M	14	F	5	L F	L F polar		L anterior frontal resection	FCD IIa
3	M	16	T	3	R T	R T	R T ganglioglioma	RT resection and lesionectomy	ganglioglioma
4	W	19	F	9	R F dorsolateral	R F dorsolateral	FCD R precentral sulcus	R F resection	gliosis
5	W	24	FTI	3	R FT	bilateral T, R > L	L T pole cyst	R FT insular resection	n.a.
Patients without FOs									
6	M	37	T	8	R T	R FT		R T resection	FCD IIa
7	M	21	TI	2	L FCP	L FCP	L T pole hypoplasia, L HS, L hemispheric atrophy	L T lobectomy plus insula	gliosis

8	M	21	Cingulate	15	L FCT	L F dorsolateral	L central cingulate lesion	L central cingulate lesionectomy	tuberous sclerosis
9	M	36	F	10	L F	L T	L F perisylvian gliosis	L orbitofrontal lesionectomy	FCD IIb
10	M	47	T	7	L FCT	L FCT	L F polymicrogyria + increase volume of L amygdala	L T resection	HS

Legend. C, central; EEG electroencephalography; F, frontal; FCD, focal cortical dysplasia; FO, fast oscillation; HS, hippocampal sclerosis; I, insula; L, left; M, man; na, not available; O, occipital; P, parietal; R, right; T, temporal; W, woman

Table 2. Depth of the epileptic generator, epileptic spikes, and fast oscillations.

#	Depth of generator	# Spikes marked	# FOs	# Spikes localized	# FOs localized	# Spikes of the consensus map	# FOs of the consensus map
Patients with FOs							
1	superficial	303	10	303	10	164	5
2	superficial	258	12	258	11	101	10
3	intermediate	155	12	155	11	69	6
4	superficial	12	20	12	20	8	6
5	superficial	20	9	20	9	10	6
Patients without FOs							
6	deep	92	4	92		33	
7	deep	42	3	42		23	
8	deep	40	3	40		20	
9	intermediate	34	2	34		22	
10	deep	40	1	40		16	

For each patient the number of marked and localizable epileptic spikes and FOs are presented. The depth of the generator is given. It is based on the available clinical information by an epileptologist. FO, fast oscillation.

FIGURES

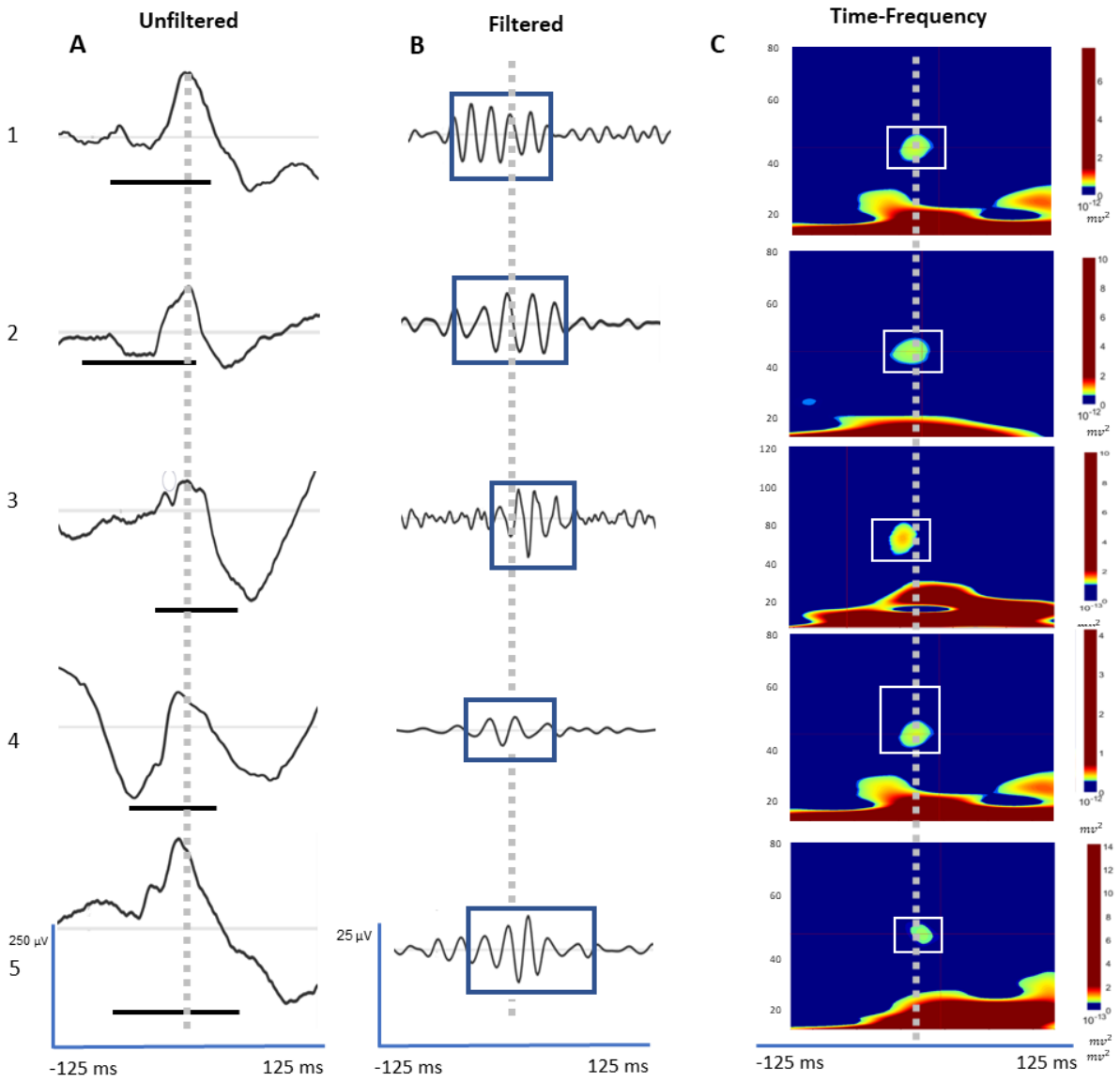

Figure 1. Detection of Fast Oscillations (FO) using scalp HD-EEG. This figure provides examples of FOs. (A) unfiltered signal showing the interictal spike (B) filtered single (40-80 Hz) demonstrating the FO event over the background (C) time frequency plot showing the isolated peak in the 40-80 Hz frequency band atop of the spike. Time scale is set to the peak of the event and 125ms before and after are given.

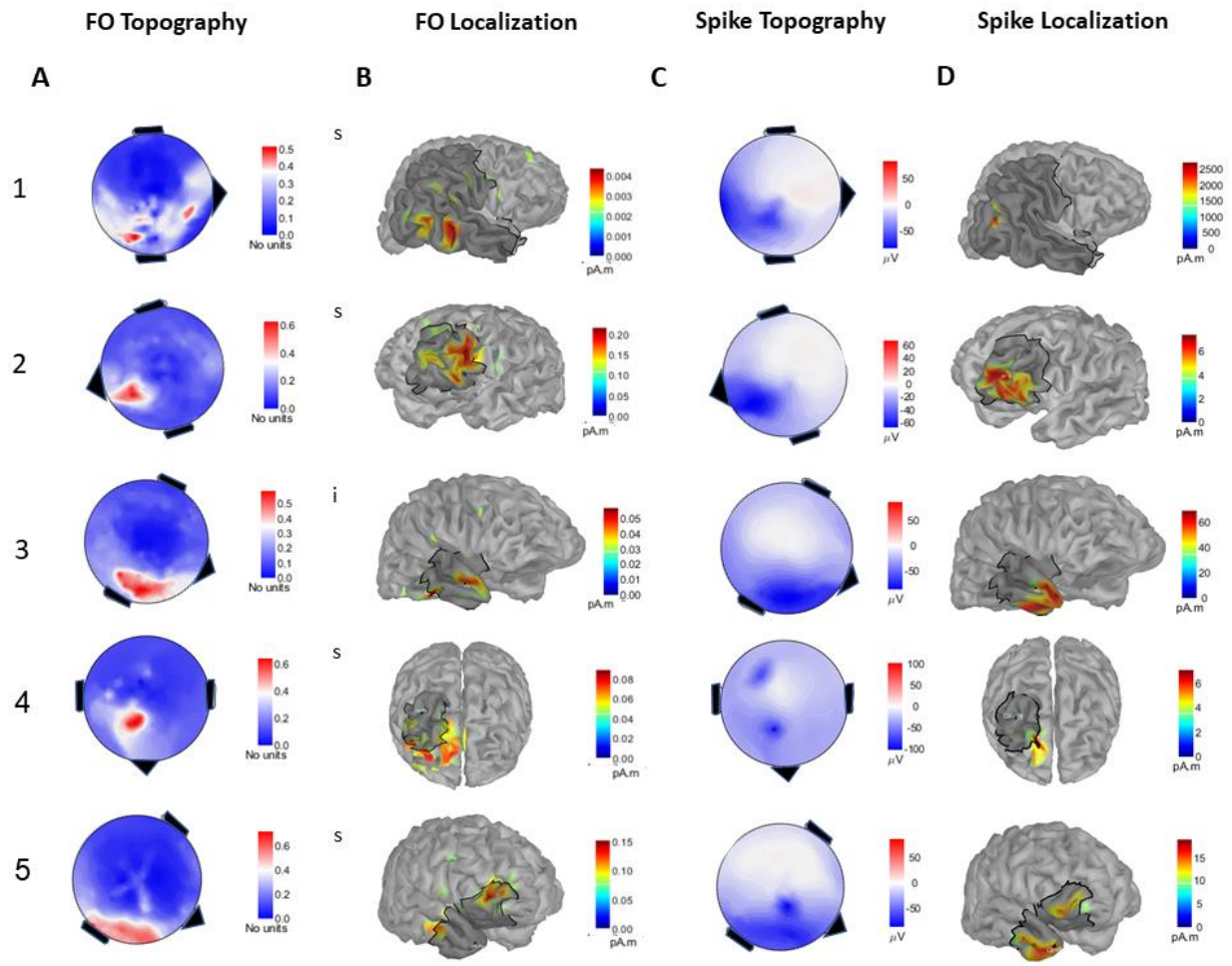

Figure 2. Results of electrical source imaging for Fast Oscillations (FO) and spikes. FOs and spikes were source localized using the Maximum Entropy on the Mean method (wavelet MEM for FOs and coherent MEM for spikes) in patients which showed > 5 FOs. The surgical cavity was fitted on the brain model and was marked as grey area. (A) mean scalp topography of the consensus map (defined as cluster exhibiting the largest amount of single events) of FOs for each patient. Power topography maps were averaged together for the peak of the event time course over the peak frequency as visualized by the TF plot (B) electrical source imaging (wMEM) of the consensus map of the FOs for each patient (C) mean topography of the consensus map of spikes for each patient (D) electrical source imaging (cMEM) of the consensus map of the spikes for each patient. Please note that scalp topographies (column A and C) are presented following the same orientation as the corresponding source maps. All source localization results are presented using a color map scaled to the maximum reconstructed intensity of the corresponding map and thresholded at 50% of their maximum

value. Note that the current amplitude of sources of FOs was as expected several orders of magnitude lower than that of spike sources as well as that patient 1's large cavity is due to a disconnecting surgery. The topographical maps are oriented to the same direction as the source localization map results.

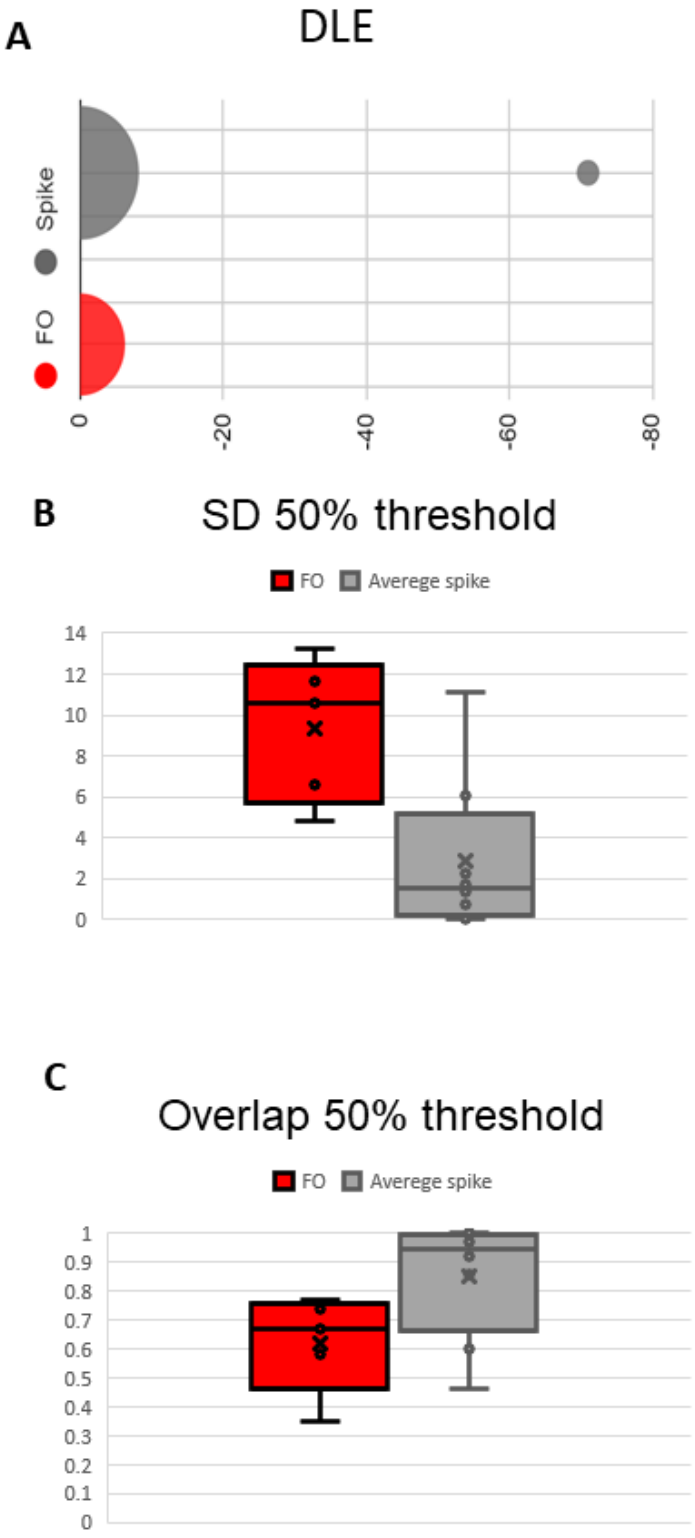

Figure 3. Validation metrics of the results of electrical source imaging of Fast Oscillations (FO) and spikes. Different measures were used to evaluate the success rate of the detectability and localization of FOs compared to spikes (A) Distance Localization Error (DLE) (Dmin) as measured from the maximum of the localization map to the closest point of the cavity (Dmin=0 mm means within cavity, Dmin is represented as a negative distance from the cavity i.e 1mm distance from the cavity is Dmin= -1mm) (B) Spatial dispersion (SD) maps (50% threshold) measuring the amount of activity outside the cavity in relation to the distance from the closest cavity point (C) Overlap between the activation maps (50% threshold) with the cavity such that 100% means that the localization map is completely localized inside the cavity.

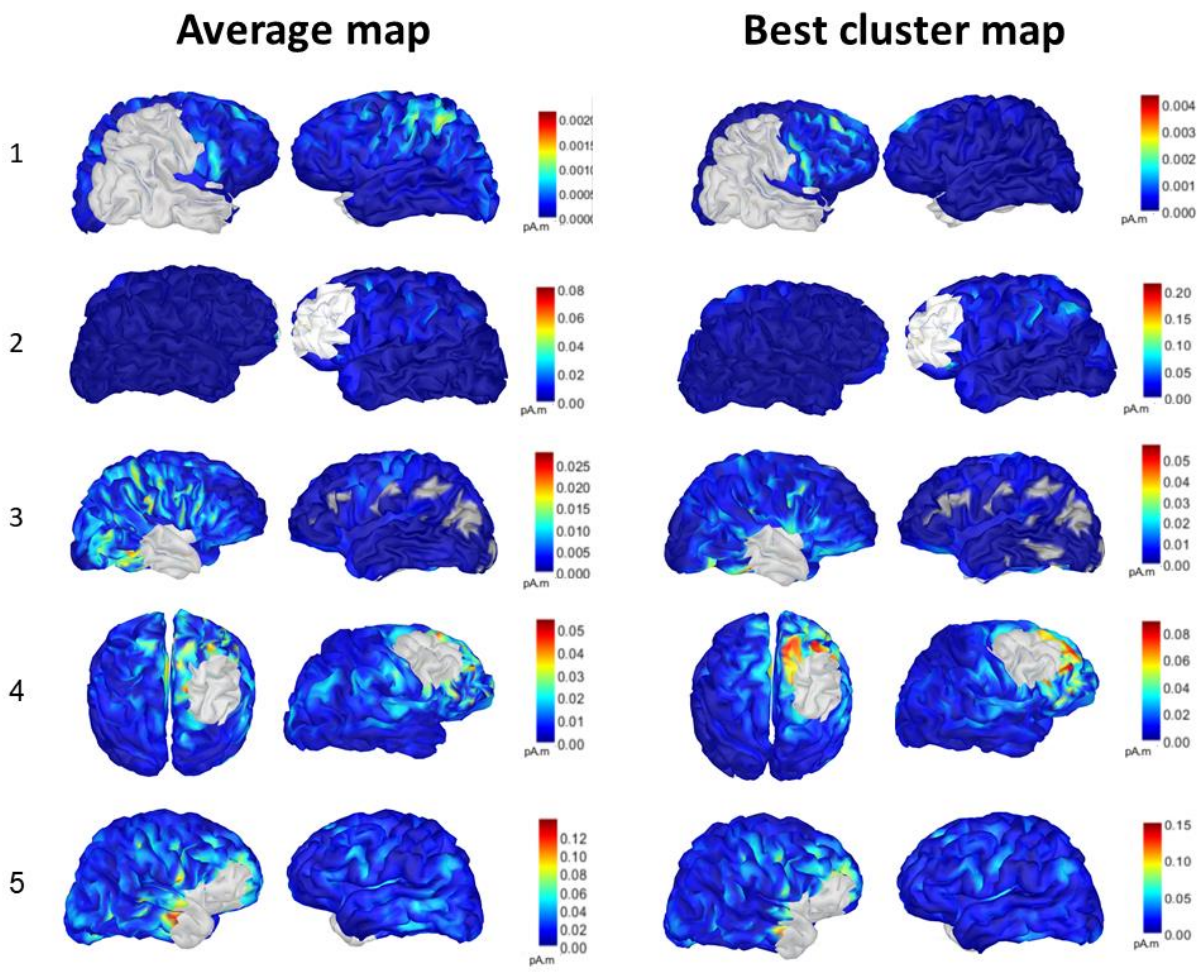

Figure 4. Comparison between electrical source imaging performed with the average vs. the consensus map FOs. FOs were clustered using hierarchical clustering. The cluster exhibiting the most events was chosen as consensus map. The cavity is marked in gray and the spurious activity outside the cavity is then depicted. Note that the maximum is inside the obscured cavity (as shown in Fig. 2) and only the spread is shown.